Journal of Cancer Research and Clinical Oncology (2021) 147:1115–1123
https://doi.org/10.1007/s00432-021-03513-w

ORIGINAL ARTICLE – CANCER RESEARCH

Investigation of a novel brachytherapy ureteral stent: trial studies on normal beagle dogs

Dechao Jiao[1] · Yuan Yao[1,2] · Kaihao Xu[1] · Qinyu Lei[1] · Zongming Li[1] · Xinwei Han[1,2] · Jianzhuang Ren[1]

Received: 14 October 2020 / Accepted: 9 January 2021 / Published online: 25 January 2021

Abstract

Purpose To evaluate the safety and feasibility of a newly designed ^{125}I brachytherapy ureteral stent (BUS) in normal dogs.
Methods A BUS loaded with 10 ^{125}I seeds (Group A: 0.8 mCi, Group B: 0.4 mCi, Group C: 0 mCi) was designed and tested in 27 normal beagle dogs. Routine blood tests, gross observations, cumulative radiation doses, tissue reaction assessed by hematoxylin–eosin/Masson staining, mRNA analysis by RT-qPCR and protein expression of Caspase-3, Collagen I, PCNA, and α-SMA were performed at 2, 4 and 8 weeks.
Results The BUS was implanted successfully in all dogs (27/27) without surgery-related death. The ureter diameter and radiation injury score increased along with radiation accumulation ($p < 0.05$). Histopathologic analysis showed necrotic tissue and lateral fibrosis to different extents in the ureteral walls that gradually increased in all groups ($p < 0.05$); however, epithelial cell proliferation in groups A and B was lighter than that in the control group ($p < 0.05$).
Conclusion Placement of the newly designed ^{125}I BUS was safe and feasible in dogs, and clinical studies are required to test its use in humans.

Keywords Ureteral stent · Brachytherapy · Animal study · ^{125}Iodine · Urinary system

Introduction

The standard treatment plan for ureteral epithelial cell carcinoma is radical kidney and ureteral plus bladder cuff resection, but this procedure causes the patient to lose a kidney. This is a difficult choice for patients with an isolated kidney, advanced age, renal insufficiency, bilateral ureteropathy, or intolerance or rejection of open surgery (So and Siddiqui 2018). The treatment of advanced ureteral cancer is mostly limited to traditional external radiotherapy; however, the radiotherapy cycle is long (60–70 Gy, 5–6 weeks), and the treatment dose is limited due to lesions close to the spinal cord, intestinal canal, and large blood vessels, which may result in spinal cord damage, intestinal injury, and retroperitoneal fibrosis (Huang et al. 2016). Brachytherapy of malignant solid tumors with radioactive ^{125}I seed has been widely used in the clinic with encouraging clinical efficacy (Li et al. 2019). Inspired by the high-dose rate radiotherapy in the ^{192}Ir cavity, our center strung radioactive ^{125}I seeds into a chain structure and placed them into the bile duct, esophagus, and portal vein tumor thrombus to achieve good clinical efficacy (Bi et al. 2020; Jiao et al. 2017; Zhang et al. 2018). This, then, raises the question of whether ^{125}I seed strand brachytherapy is suitable for malignant ureteral obstruction. Theoretically, the ureter is a long, thin tube-shaped structure, and when the tumor is very small (5–10 mm), it can cause ureteral obstruction and hydrops. The irradiation distance of ^{125}I seeds is within 1.7 cm, which may play a better role in intraluminal low-dose brachytherapy therapy (ILBT). To address ureteral obstruction and ILBT synchronously, a

Dechao Jiao and Yuan Yao contributed equally to this work.

Supplementary Information The online version contains supplementary material available at https://doi.org/10.1007/s00432-021-03513-w.

✉ Xinwei Han
13592583911@163.com

✉ Jianzhuang Ren
rjzjrk@126.com

[1] Department of Interventional Radiology, The First Affiliated Hospital of Zhengzhou University, Zhengzhou 1 Jianshe Road, Zhengzhou 450052, Henan, People's Republic of China

[2] Academy of Medical Sciences, Zhengzhou University, Zhengzhou 450052, Henan, People's Republic of China

newly designed ^{125}I brachytherapy ureteral stent (BUS) with dual cavities was developed in our center, and it can serve the dual roles of urine drainage and brachytherapy. The aim of this study was to verify its safety and feasibility in healthy animals to provide a basis for further clinical use.

Materials and methods

Development of the BUS

The size of the ^{125}I BUS was 20 cm in length and 7 French in diameter with a double J structure at both ends (Tuoren Co. Ltd., Henan, China, Fig. 1), and it has double cavities (drainage cavity and ^{125}I seed cavity) without communication with each other. The drainage cavity and seed cavity have an opening hole 5 cm away from the head end that serves as a seed implantation channel. Every newly designed BUS can load 10 ^{125}I seeds, and the nonseed part was threaded with a 0.018-inch guidewire (Cook Inc., Bloomington, IN, USA). The ^{125}I seeds (Saide Biological Technology Co., Ltd., Tianjin, China) have a size of 0.8 mm × 4.8 mm (diameter × length) with a half-life of 59.6 days; moreover, they have energies of 35.5 keV (γ-ray) and 27.4–31.5 keV (X-ray), an initial dose rate of 7.7 cGy/h and an irradiation distance of 17 mm.

Animal experiment

The animal study was approved by the Institutional Animal Care and Use Committee of Zhengzhou University. Twenty-seven healthy beagle dogs (male: 14, female: 13, weighing 15–16 kg) were randomly divided into three groups (group A: BUS loaded with 0.8 mCi/^{125}I; group B: BUS loaded with 0.4 mCi/^{125}I; group C: BUS loaded with 0 mCi/^{125}I; 9 dogs per group). The contralateral ureter was used as a control group. After successful anesthesia [intravenous injection of 3% pentobarbital sodium (30–35 mg/kg)], the animal was placed in the supine position with the limbs fixed for skin preparation and disinfection of the lower abdomen. After a midline incision of the lower abdomen, the bladder wall of the dog was cut 2 cm longitudinally, and both ureters were separated. Under fluoroscopic (Artis Zeego; Siemens, Germany) guidance, with the help of a guidewire, a 5F catheter (Boston Scientific, Natick, MA, USA) was retrogradely introduced into the ureter and renal pelvis, and then it was replaced with a newly designed BUS with both stent ends located in the renal pelvis and bladder. The other side of the ureter remained in the normal condition and served as the control group. If the bladder incision was too large, it was wrapped with omentum and sutured. All wounds recovered well. According to the plan, three dogs were randomly killed by air embolism, and routine blood, liver function, renal function, and tissue reaction tests were performed.

Serum biochemical examination

Three milliliters of blood was collected from the radial vein of the forelimb before 1, 2, 4 and 8 weeks, and appropriate anticoagulants were added at the same time. Then routine blood tests were carried out by an automatic blood cell counter. The remaining blood was put into a 5-ml centrifuge tube, placed in a 37 °C water bath for 15 min, and then centrifuged at 3000 r/min for 15 min. Biochemical tests, including routine blood tests and liver and renal function analysis, were performed with an automatic biochemical analyzer.

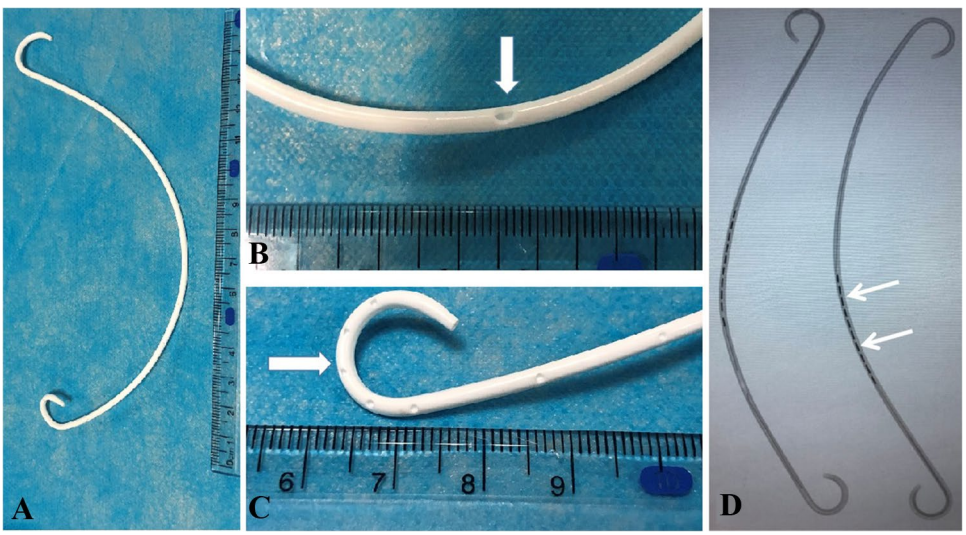

Fig. 1 **a** A newly designed BUS has a double cavity (drainage cavity and 125I seed cavity) without communication with each other; **b** An opening hole 5 cm away from the head end serves as the seed implantation channel; **c** The side holes at both BUS ends are used for urine drainage; **d** BUS under fluoroscopy, 125I seeds were directed by white arrows

Imaging examination and gross observation

Whole abdomen single-photon emission computed tomography (SPECT) was performed 3 days after the operation to observe γ ray distribution, seed loss or displacement. According to the experimental plan, the intact kidney ureter bladder was separated, and photos were taken at different time points. The renal pelvis and upper ureter were incised longitudinally to observe hydronephrosis and the ureter internal surface for signs, such as bleeding, perforation, rupture, and ulceration.

Hematoxylin–eosin and Masson staining

Cross-sectional specimens of the BUS area were obtained and fixed with formalin for further hematoxylin–eosin (HE) staining at 2, 4, and 8 weeks after the beginning of the experiment. Submucosal inflammatory cell (lymphocyte and neutrophil) infiltration, epithelial cell layer thickness, collagen deposition, granulation tissue proliferation, and ureteral wall fibrosis were investigated according to histological scoring standards (Table 1). Masson staining was performed to further understand the extent of fibrosis.

Real-time fluorescent quantitative PCR

Total RNA was extracted from fresh tissues with TRIzol reagent (Invitrogen, Carlsbad, CA, USA). The concentration and quality of RNA were verified by a Nanodrop nd-1000 spectrophotometer (Nanodrop Technologies, USA). The extracted RNA was reverse transcribed with a Takara reverse transcription kit (Takara, Dalian, China). The expression levels of PCNA, collagen and caspase-3 were detected with a SYBR Green PCR Master Mix kit. With β-actin serving as an internal reference, the relative expression of these mRNAs was calculated by the $2-\Delta\Delta CT$ method (Table S1).

Immunohistochemistry

Cross-sectional specimens of the BUS area were obtained and embedded in a wax block, and PCNA, collagen, caspase-3 and α-SMA testing was performed to observe the difference in protein expression in tissues and cells at 2, 4, and 8 weeks after the beginning of the experiments. The optical density calculated by ImageJ Pro software indirectly reflected the protein expression, and the statistical results were compared directly.

Western blot

The total protein of the tissue was extracted by radioimmunoprecipitation assay (RIPA) buffer, and then the protein was quantified by a BCA protein quantitative kit, separated by 10% SDS polyacrylamide gel, transferred to PVDF membrane, and blocked in 5% skim milk (diluted in TBST). Then PCNA, collagen and Caspase-3 antibodies were diluted according to their respective dilution ratios, and the membranes were incubated with the appropriate primary antibodies at 4 °C. After washing three times with TBST, the membranes were incubated in horseradish peroxidase (HRP)-bound secondary antibody (1:500) at room temperature for 1 h. After washing with TBST three times, the bands were exposed with enhanced chemiluminescence (ECL) hypersensitive luminescent solution (EpiZyme, Shanghai, China) and visualized with an Amersham imager 600 (Cytiva, USA).

Radiation dosimetry

The tissue-absorbed doses of radiation 5 and 10 mm transverse from the BUS at different times in the 0.4 and 0.8-mCi groups were calculated using the following equation[7–9]: $D_\gamma = 34.6(\Sigma\ \Delta i\phi i)\ C0Teff[1—e\text{-}(0.693/Teff)t]\Delta i$. Since iodine 125 seeds emit gamma rays, the following formula can be used to calculate the absorbed dose (Homs et al. 2003; Stabin et al. 1999). $D_\gamma = 34.6\ (\Delta\ I\ \phi\ I)\ c0teff\ [1\text{-}E\text{-}(0.693/teff)\ t]$, Δ I represents the constant absorbed dose, ϕ I represents the energy proportion of target absorption,

Table 1 Histological scoring standard

Index	Score			
	0	1	2	3
Epithelium detachment	None	< 1/3	1/3–2/3	> 2/3
Capillary dilatation and congestion	Absent	Mild	Moderate	Marked
Lymphocytic infiltration	Absent	Focal scattered	Focal dense	Dense
Neutrophil infiltration	Absent	Focal scattered	Focal dense	Dense
Submucosal gland	Normal	Swelling	Atrophy	Necrosis
Erythrocyte exudation	Absent	Mild	moderate	Marked
Cartilage necrosis	Absent	< 1/3	1/3–2/3	> 2/3

iodine 125 seeds, which are 0.219, C0 is the radiation dose in tissues when t = 0 μCI/g, and TEFF is the physical half-life of ^{125}I seeds.

Statistical analysis

SPSS 20.0 software (IBM) was used for statistical analysis. Continuous data are presented as the mean ± standard deviation. A *t* test was used to compare the normally distributed data of two groups, one-way ANOVA was used for data of all groups, the least significant differences (LSD) method was used for pairwise comparisons of intra- and among-group comparisons, and the Mann–Whitney *U* test was used for rate comparisons. Repeated measures analyses of variance were used to compare repeated data. $P < 0.05$ was statistically significant.

Results

Blood routine and blood biochemistry

After stenting, the experimental animals in the 0.8-mCi group showed increased white blood cells (WBCs) at 1 week ($p < 0.05$), which returned to normal at 2, 4, and 8 weeks, but WBCs showed no significant change in the 0.4-mCi and 0 m-Ci groups at 1, 2, 4, or 8 weeks. Hemoglobin and platelets were maintained within the normal reference range in all groups. Blood biochemical analysis (including alanine aminotransferase, aspartate aminotransferase, total cholesterol, triglyceride, total bilirubin, direct bilirubin, urea nitrogen, creatinine, blood glucose, total protein, albumin, globulin, and urea nitrogen) was maintained within the normal range at 1, 2, and 4 weeks (Table 2).

Gross specimens

Postoperative SPECT at day 3 showed precise γ-ray coverage and no BUS displacement. All ureters with BUS showed different degrees of hydronephrosis, and there was a trend of aggravation as time went on; however, there was no hydronephrosis in the contralateral ureter in any group (Fig. 2). The BUS located at the upper or end of the renal pelvis (without the seed part) showed no serious damage. We focused on the gross specimens of the 0.8-mCi group with a higher risk of radiation injury (Fig. 3), showing that the ureter diameter gradually thickened and that the wall gradually thickened over time (Table 3).

HE and Masson staining

Compared with those in the control group, the ureteral injury scores gradually increased over time in the treatment groups ($p < 0.05$) (Table 4). Two weeks after the

Table 2 Blood indexes of 0.8-mCi animal group at different time

Index (unit)	Baseline	1 week	2 weeks	4 weeks	8 weeks	Reference range
Red blood cells (10^6/μL)	6.90 ± 0.50	7.00 ± 0.39	6.81 ± 0.31	6.20 ± 0.28	6.36 ± 0.49	5.57 ~ 7.82
White blood cell (10^3/μL)	10.51 ± 2.05	13.26 ± 1.03[a]	10.09 ± 2.14	10.67 ± 2.24	10.51 ± 0.88	5.81 ~ 14.71
Platelets (10^3/μL)	271.22 ± 72.19	326.6 ± 20.26	297.6 ± 62.95	283.6 ± 36.60	292.4 ± 15.54	175.35 ~ 484.28
Hemoglobin(g/dL)	14.42 ± 1.34	15.14 ± 1.13	14.29 ± 1.08	14.00 ± 0.73	14.16 ± 0.72	11.95 ~ 17.68
Alanine aminotransferase (U/L)	28.6 ± 5.60	28.8 ± 5.47	30.7 ± 4.52	30.46 ± 7.46	30.81 ± 4.71	14.52 ~ 39.85
Aspartate aminotransferase (U/L)	36.4 ± 5.76	34.7 ± 4.18	36.7 ± 4.94	32.91 ± 3.15	38.94 ± 1.43	21.32 ~ 48.41
Total cholesterol (mmol/L)	4.15 ± 0.86	4.71 ± 0.64	4.58 ± 0.65	4.19 ± 0.53	4.45 ± 0.92	2.75 ~ 5.78
Triglyceride (mmol/L)	0.53 ± 0.12	0.57 ± 0.10	0.52 ± 0.15	0.61 ± 0.08	0.57 ± 0.16	0.54 ± 0.15
Total bilirubin (μmol/L)	1.55 ± 0.74	1.36 ± 0.55	1.43 ± 0.53	1.45 ± 0.71	1.61 ± 0.44	0.31 ~ 2.65
Direct bilirubin (μmol/L)	0.99 ± 0.51	1.05 ± 0.66	0.92 ± 0.47	0.94 ± 0.51	0.86 ± 0.38	0.01 ~ 1.85
Urea nitrogen (mmol/L)	4.27 ± 0.81	4.35 ± 1.08	4.83 ± 0.67	5.32 ± 0.09	5.81 ± 0.27	1.98 ~ 5.66
Creatinine (μmol/L)	40.8 ± 7.66	42.6 ± 7.27	43.1 ± 7.38	47.05 ± 4.00	49.01 ± 6.24	26.81 ~ 55.31
Blood glucose (mmol/L)	5.78 ± 0.43	5.85 ± 0.69	5.69 ± 0.52	5.88 ± 0.63	5.64 ± 0.80	4.87 ~ 6.81
Total protein (g/L)	56.8 ± 4.26	56.2 ± 3.93	55.7 ± 4.38	55.01 ± 5.21	55.09 ± 1.62	48.94 ~ 65.74
albumin (g/L)	31.5 ± 3.01	31.5 ± 2.79	31.2 ± 2.44	30.81 ± 1.96	31.19 ± 0.70	27.63 ~ 37.75
Globulin (g/L)	24.8 ± 2.26	23.5 ± 2.45	23.5 ± 3.36	25.98 ± 1.48	25.67 ± 1.00	18.25 ~ 28.59

[a]White blood cell (baseline vs. 1 week) $p < 0.05$

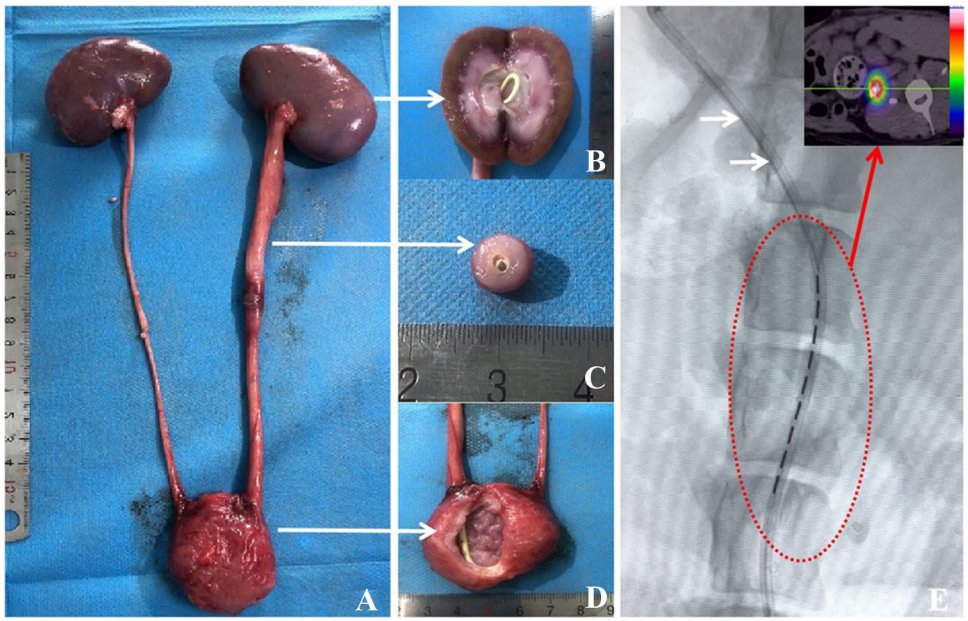

Fig. 2 **a** Compared with the contralateral volume, the kidney and ureter volume increased significantly, and ureter dilation and hydronephrosis were observed at 8 weeks after BUS implantation in the 0.8-mCi group; **b** the kidney color was normal, and the collecting system was dilated; **c** The cross-section of the BUS with the 125I segment of the ureter and drainage cavity was blocked by epithelial cells and stones; **d** No bladder mucosal hyperplasia and other secondary changes in the BUS bladder part; **e** BUS implantation under fluoroscopy, BUS irradiation distribution showed good SPECT at 3 days after operation

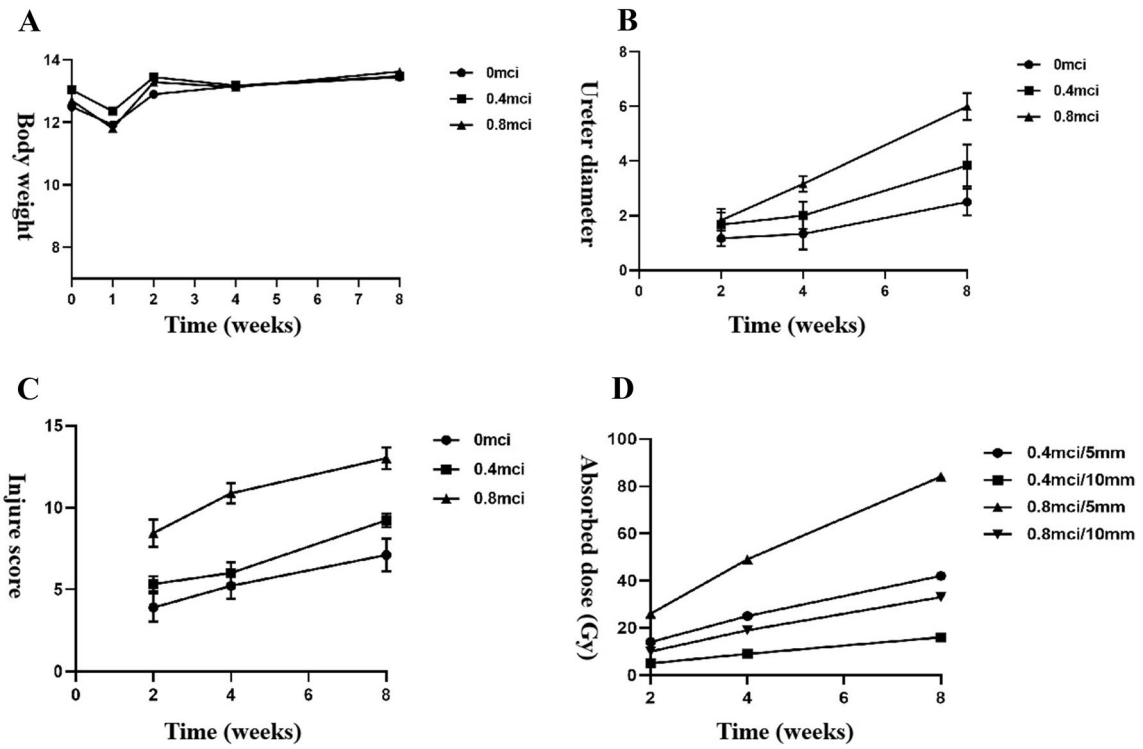

Fig. 3 Body weight, ureteral diameter, injury score, and absorption dose at different time points

operation, the main manifestations were epithelial cell rupture, local tissue edema and telangiectasia; at 4 weeks, granulation tissue hyperplasia and local fibrosis were observed; at 8 weeks, obvious fibrosis and muscle layer thickening were observed in all groups, which was prominent in the 0.8-mCi group. For Masson staining, there was no obvious proliferation of collagen fibers and muscle fibers at 2 weeks; the proliferation of collagen fibers was more obvious at 4 weeks; and the proliferation of muscle fibers was most obvious at 8 weeks. Epithelial cell proliferation of groups A and B was lighter than that of the control groups (Fig. 4).

Table 3 Ureter diameter changes at all group

Group	Ureter diameter (mm)		
	2 weeks	4 weeks	8 weeks
0-mci group	1.17 ± 0.24	1.33 ± 0.74	2.50 ± 0.41
0.4-mci group	1.67 ± 0.47	2.00 ± 0.41	3.83 ± 0.62
0.8-mci group	1.83 ± 0.24	3.17 ± 0.24	6.00 ± 0.41

LSD was used for pairwise comparison. The results showed that there were statistically significant differences in the comparison (dose, time) among the groups ($p < 0.05$)

Table 4 Tissue scores of groups at different times

Group	Injury score		
	2 weeks	4 weeks	8 weeks
0-mci group	3.89 ± 0.87	5.22 ± 0.79	7.11 ± 0.99
0.4-mci group	5.33 ± 0.47	6.00 ± 0.67	8.56 ± 0.83
0.8-mci group	8.44 ± 0.83	10.87 ± 0.63	13.00 ± 0.67

LSD was used for pairwise comparison. The results showed that there were statistically significant differences in the comparison (dose, time) among the groups ($p < 0.05$)

Real-time quantitative PCR and Western blot analysis

Compared with that in the control group, the expression of mRNA and protein levels increased gradually over time in the treatment groups and showed statistical significance ($p < 0.05$). At the same time point, the expression of PCNA was lowest in the 0.8-mCi group, especially at 8 weeks. The mRNA and protein expression levels of α-SMA, collagen I protein and caspase-3 protein were highest in the 0.8-mCi group and lowest in the 0-mCi group at 2, 4, and 8 weeks, respectively ($p < 0.05$) (Fig. 5).

Immunohistochemistry

Compared with that in the control group, the expression of PCNA, α-SMA, collagen I protein and caspase-3 protein increased gradually over time in the treatment groups and showed statistical significance ($p < 0.05$). At the same time point, the expression of PCNA was lowest in the 0.8-mCi group, especially at 8 weeks. The expression of α-SMA, collagen I protein and caspase-3 protein were highest in the 0.8-mCi group and lowest in the 0-mCi group at 2, 4, and 8 weeks, respectively (Fig. 6).

Radiation dosimetry

The absorbed radioactive dosages of the tissues adjacent to the BUS at distances of 5 and 10 mm (reference point) from the BUS are listed in Table 5. The highest cumulative dose in the 0.8-mCi group was 84.29 Gy at 8 weeks.

Discussion

The reason for radical resection of ureteral carcinoma (UC) of the bladder and ureter resection is the renal pelvis, ureter and bladder all originate from the mesoderm, and the morphology and biological behavior are similar. The recurrence of UC after unilateral upper urinary tract tumor resection is 15–50%, and even as high as 70% (Campi et al. 2019; Rouprêt et al. 2015). The operation is traumatic, and patients need to lose one kidney. This is a challenge for patients with an isolated kidney, old age, or renal insufficiency and for those who refuse or cannot undergo surgical resection. Therefore, more minimally invasive therapies for ureteral malignancies are urgently needed in clinical practice.

The minimally invasive clinical treatment of malignant tumors by interstitial puncture and implantation of ^{125}I seeds has become a common technique. The question then is whether radioactive particle brachytherapy is suitable for cavitary organs such as the ureter. It has been reported that

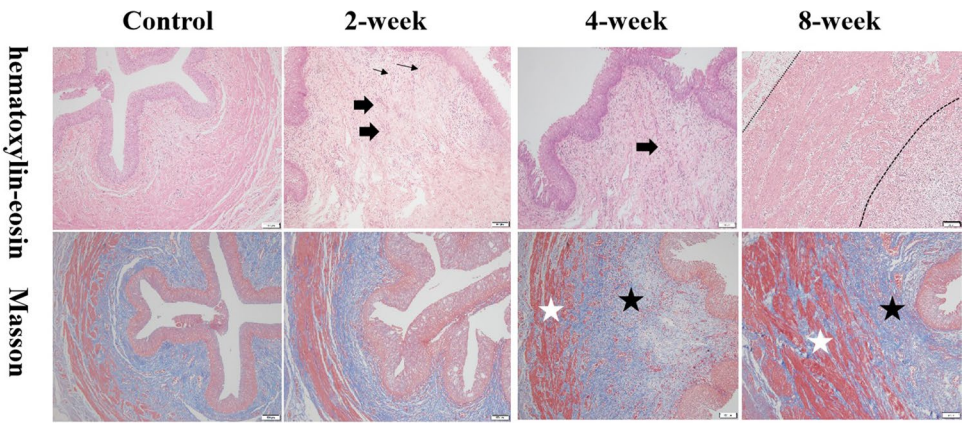

Fig. 4 Histopathological and Masson's trichrome staining at different time points in the 0.8-mCi group (100×). Large black arrow: interstitial edema; small black arrow: telangiectasia; large white arrow: granulation tissue formation; double dashed line: muscle layer thickening; black five-pointed star: collagen fiber hyperplasia; white five-pointed star: muscle fiber hyperplasia

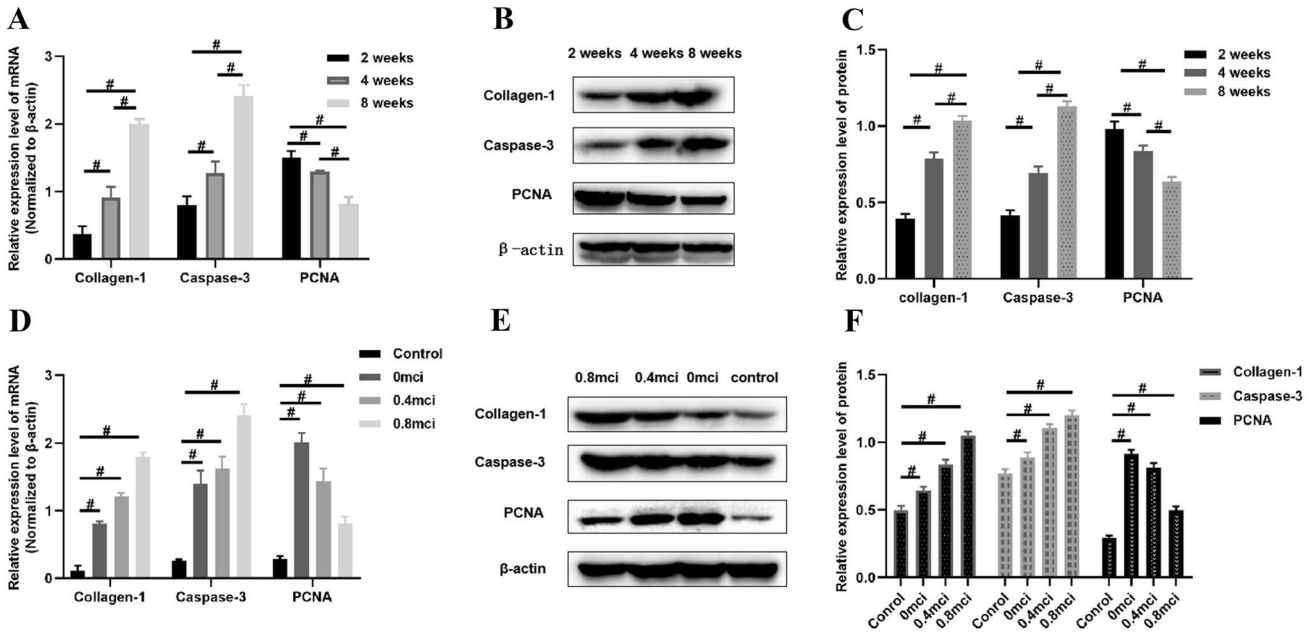

Fig. 5 RT-PCR and Western blot analysis of collagen-1, caspase-3 and PCNA expression (#, $p < 0.05$)

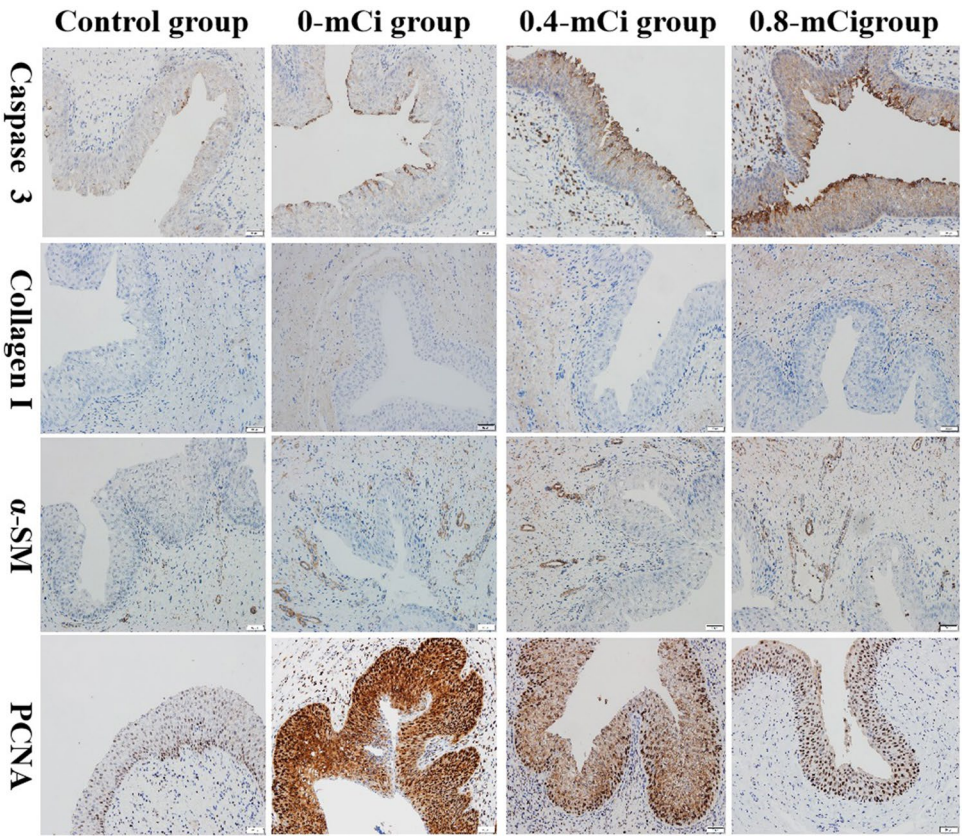

Fig. 6 Immunohistochemistry of caspase 3, collagen I, PCNA, and α-SMA in all groups at 8 weeks (100×). The expression of α-SMA, collagen I protein and caspase-3 protein were highest, and PCNA was lowest in the 0.8-mCi group

^{125}I seeds have been stranded into a line structure within a catheter to treat bile duct obstruction and portal vein tumor thrombus with satisfactory clinical results (Hu et al. 2019; Wu et al. 2018). A BUS, which had the characteristics of local high-dose accumulation and minimal damage to surrounding tissues, was developed to fulfill both drainage and

Table 5 Absorbed radioactive dosages of the tissues adjacent to the stent at a distance of 5 and 10 mm from UBS

Group	Absorbed dosage (5 mm from UBS, Gy)			Absorbed dosage (10 mm from UBS, Gy)		
	2 weeks	4 weeks	8 weeks	2 weeks	4 weeks	8 weeks
0.4-mCi group	14.07	25.24	41.78	5.40	9.38	15.92
0.8 mCi group	25.66	49.41	84.29	10.33	18.96	33.43

brachytherapy functions. Notably, the longer strand structure can inhibit tumor implantation metastasis. This is the first report to test its safety and feasibility in healthy beagle dogs.

The technical success rate of retrograde implantation of the newly designed BUS was 100%. All 27 experimental animals were euthanized and tested in accordance with the experimental plan. Except for the weight loss of animals within the first week after the experiment, the condition of the experimental animals at other times during the experiment was the same as that of normal dogs, indicating that ^{125}I brachytherapy is a safe local treatment without obvious effect on the whole body. The WBCs of the experimental animals in the 0.8-mCi group increased temporarily for 1 week and then returned to normal. Considering that the initial animals in this experiment were part of the 0.8-mCi group, the operator was slightly inexperienced, resulting in long operation times, which means more damage.

From the gross specimen and pathological results, the implantation time and ^{125}I seed activity were the main promoting factors of ureteral fibrosis and apoptosis. The results of animals in the 0-mCi group showed that fibrosis and apoptosis of ureteral tissue gradually increased with time, but the degree was weaker than that of the 0.4-mCi and 0.8-mCi groups at the same time point, especially at the 8-W time point, which indicated that both stent and ^{125}I brachytherapy could cause a certain degree of fibrosis. However, the local proliferation caused by stent stimulation in the early stage of BUS played a major role. As time went on, the local cumulative dose increased, and the proliferative ability of epithelial cells was inhibited to some extent, although the fibrosis in the submucosa became increasingly obvious because of brachytherapy, which can explain why the diameter of the ureter reached 2.5 and 6.0 mm at 8 weeks in the 0-mCi and 0.8-mCi groups, respectively, so withdrawal of the BUS is suggested after finishing ^{125}I brachytherapy. Liu et al. (2007) tested a newly designed irradiation stent on the bile duct of normal animals with prescription doses of 50, 100, 150, and 200 Gy and found that the stents were surrounded by necrotic tissues and lateral fibrous tissues with cumulative dose accumulation. Moreover, ^{125}I brachytherapy on the radiation injury of nerves (Jiao et al. 2014), blood vessels (Zhang et al. 2016), the trachea (Wang et al. 2017) and so on has also been reported in the past, and all results showed slight or no injury to the target or surrounding organs. This was mainly due to the dose of radiation administered by the 125I radioactive source decreases rapidly with distance, which gave the surrounding normal tissues time to fully mobilize their own ability to repair.

The above results were verified by immunohistochemistry, Western blot and qRT-PCR. Therefore, the radiation dose is the most important index for evaluating safety. The 0.8-mCi group is 84.29 Gy (8 weeks) at the 5 mm dose reference point, which exceeded the conventional external radiotherapy dose (60–70 Gy), indicating that BUS is expected to achieve a radical dose for UC. Moreover, if ^{125}I brachytherapy can be completed at home, patients do not need to make appointments for conventional radiotherapy, which saves social medical resources and costs. Furthermore, it was 33.43 Gy at the 10 mm dose reference point, a decrease of 60.03% of the dose comparing with that of the 5 mm dose reference point, which will minimize the damage to surrounding normal tissues.

In the 0.8-mCi group, ureteral injury (13.00 ± 0.67) and the largest ureteral diameter (6.00 ± 0.41) were observed at 8 weeks. Considering the aggravation of local epithelial cell detachment, the aggravation of mucosal basal fibrosis, the decrease in ureteral peristalsis, and the limitation of descending urine, as well as secondary urinary stones in the drainage tube, the drainage cavity of the BUS was blocked, and the ureteral dilatation and hydronephrosis were aggravated, which may be due to blockage factors and an increase in the renal pressure in the drainage channel decreasing drainage efficiency. In the 0.8-mCi group, the cumulative dose increased, and tissue exfoliation increased. Therefore, it is suggested that the BUS should be removed or replaced within 8 weeks. Masson staining further revealed the development of fibrosis, that is, the proliferation of collagen fibers, and finally an increase in muscle fibers. This development and evolution mechanism needs further research.

There are still some limitations to this study. For example, there is no model of ureteral tumor that would better show the effects of the BUS on tumor masses. Second, considering that ureters of dogs are smaller than those of humans and that the diameter of the newly designed BUS is smaller, it cannot reflect the real injury to humans. The diameter of the new stent does not match the beagle dog ureter and easily causes mechanical damage. For the new stent, there are many parts that can be optimized, such as adding special material coatings to strengthen its compliance and cause less friction and damage, adding drug coatings to achieve local

chemotherapy on the basis of drainage and radiotherapy, and applying radiotherapy sensitizers to further increase the curative effect of radiotherapy.

In conclusion, this newly designed BUS is safe and technically feasible in animals. It should be emphasized that the BUS implantation or replacement time is less than 8 weeks, and 0.8 mCi ^{125}I can be used to increase the radiation dose, resulting in mild damage to the normal ureter. Clinical studies will be required to test its use in humans.

Funding This work was supported by the Key Scientific Research Projects of Higher Education Institutions in Henan Province [Grant number: 20A320024].

Compliance with ethical standards

Conflict of interest The authors declare that they have no conflict of interest.

Ethics approval This study was approved by the Ethics Committee of the Affiliated Hospital of Zhengzhou University, Henan, People's Republic of China.

References

Bi Y, Zhu X, Yu Z, Jiao D, Yi M, Han X, Ren J (2020) Radioactive feeding tube in the palliation of esophageal malignant obstruction. Radiol Med (Torino) 125:544–550. https://doi.org/10.1007/s11547-020-01151-9

Campi R et al (2019) Robotic radical nephroureterectomy and segmental ureterectomy for upper tract urothelial carcinoma: a multi-institutional experience. World J Urol 37:2303–2311. https://doi.org/10.1007/s00345-019-02790-y

Homs MY, Eijkenboom WM, Coen VL, Haringsma J, van Blankenstein M, Kuipers EJ, Siersema PD (2003) High dose rate brachytherapy for the palliation of malignant dysphagia. Radiother Oncol 66:327–332. https://doi.org/10.1016/s0167-8140(02)00410-3

Hu X et al (2019) Inflammation-based prognostic scores in patients with extrahepatic bile duct lesions treated by percutaneous transhepatic biliary stenting combined with (125)I seeds intracavitary irradiation Clinical & translational oncology : official publication of the Federation of Spanish Oncology Societies and of the National Cancer Institute of Mexico 21:665–673 doi:https://doi.org/10.1007/s12094-018-1969-2

Huang YC, Chang YH, Chiu KH, Shindel AW, Lai CH (2016) Adjuvant radiotherapy for locally advanced upper tract urothelial carcinoma. Sci Rep 6:38175. https://doi.org/10.1038/srep38175

Jiao et al (2014) Implanting iodine-125 seeds into rat dorsal root ganglion for neuropathic pain: neuronal microdamage without impacting hind limb motion. Neural Regen Res 9:1204–1209. https://doi.org/10.4103/1673-5374.135326

Jiao D, Wu G, Ren J, Han X (2017) Study of self-expandable metallic stent placement intraluminal (125)I seed strands brachytherapy of malignant biliary obstruction. Surg Endosc 31:4996–5005. https://doi.org/10.1007/s00464-017-5481-5

Li Q, Liang Y, Zhao Y, Gai B (2019) Interpretation of adverse reactions and complications in Chinese expert consensus of Iodine-125 brachytherapy for pancreatic cancer. J Cancer Res Ther 15:751–754. https://doi.org/10.4103/jcrt.JCRT_884_18

Liu Y et al (2007) A novel approach for treatment of unresectable pancreatic cancer: design of radioactive stents and trial studies on normal pigs Clinical cancer research : an official journal of the American Association for. Can Res 13:3326–3332. https://doi.org/10.1158/1078-0432.ccr-07-0154

Rouprêt M et al (2015) European Association of Urology Guidelines on Upper Urinary Tract Urothelial Cell Carcinoma: 2015 update. Eur Urol 68:868–879. https://doi.org/10.1016/j.eururo.2015.06.044

So C, Siddiqui MM (2018) Urothelial carcinoma. N Engl J Med 378:e8. https://doi.org/10.1056/NEJMicm1709216

Stabin MG, Tagesson M, Thomas SR, Ljungberg M, Strand SE (1999) Radiation dosimetry in nuclear medicine. Applied radiation and isotopes: including data, instrumentation and methods for use in agriculture, industry and medicine 50:73–87 doi:https://doi.org/10.1016/s0969-8043(98)00023-2

Wang Y et al (2017) A novel self-expandable, radioactive airway stent loaded with (125)I seeds: a feasibility and safety study in healthy beagle dog. Cardiovasc Interv Radiol 40:1086–1093. https://doi.org/10.1007/s00270-017-1639-8

Wu YF et al (2018) Stents combined with iodine-125 implantation to treat main portal vein tumor thrombus. World J Gastrointest Oncol 10:496–504. https://doi.org/10.4251/wjgo.v10.i12.496

Zhang W et al (2016) Brachytherapy with Iodine-125 seeds strand for treatment of main portal vein tumor thrombi: an experimental study in a rabbit model. Am J Cancer Res 6:587–599

Zhang ZH et al (2018) Treatment of hepatocellular carcinoma with tumor thrombus with the use of iodine-125 seed strand implantation and transarterial chemoembolization: a propensity-score analysis. J Vasc Interv Radiol 29:1085–1093. https://doi.org/10.1016/j.jvir.2018.02.013